

# Charging Mechanisms of Trapped, Element-Selectively Excited Nanoparticles by Soft X-Rays

M. Grimm<sup>1,2,7</sup>, B. Langer<sup>1,2</sup>, S. Schlemmer<sup>3</sup>, T. Lischke<sup>4</sup>, U. Becker<sup>4</sup>, W. Widdra<sup>5</sup>, D. Gerlich<sup>6</sup>, R. Flesch<sup>1</sup>, and E. Rühl<sup>1</sup>

<sup>1</sup> *Institut für Physikalische Chemie, Universität Würzburg, Am Hubland, 97074 Würzburg, Germany*

<sup>2</sup> *Max-Born-Institut für Nichtlineare Optik und Kurzzeitspektroskopie, Max-Born-Str. 2a, 12489 Berlin, Germany*

<sup>3</sup> *Fakultät für Physik, Universität zu Köln, Zùlpicher Str. 77, 50937 Köln, Germany*

<sup>4</sup> *Fritz-Haber-Institut der Max-Planck-Gesellschaft, Faradayweg 4-6, 14195 Berlin, Germany*

<sup>5</sup> *Fachbereich Physik, Universität Halle-Wittenberg, 06099 Halle, Germany*

<sup>6</sup> *Institut für Physik, Technische Universität Chemnitz, Reichenhainer Str. 70, 09107 Chemnitz, Germany*

<sup>7</sup> *present address: University College Dublin, Department of Experimental Physics, Belfield, Dublin 4, Ireland*

(Dated: August 11, 2005)

The charging mechanisms of trapped, element-selectively excited free SiO<sub>2</sub> nanoparticles by soft X-rays are reported. The charge state of the particles is measured and the electron emission probability is derived. Changes in electron emission processes as a function of photon energy and particle charge are obtained from the charging current. This allows us to distinguish contributions from primary photoelectrons, Auger electrons, and secondary electrons. Processes leading to no change in charge state after absorption of X-ray photons are identified. O 1s-excited silica particles of low charge state indicate that the charging current follows the inner-shell absorption. In contrast, highly charged SiO<sub>2</sub> nanoparticles are efficiently charged by resonant Auger processes, whereas direct photoemission and normal Auger processes do not contribute to changes in particle charge. These results are discussed in terms of a simple electrostatic model.

PACS numbers: 73.22.f, 78.70.Dm

Nanoparticles cover the size regime between clusters and macroscopic condensed matter. Their unique electronic, structural, and chemical properties have been subject of numerous recent works, where the particles are studied either in solution or they are deposited on substrates [1]. Recent work also includes investigations by soft X-ray spectroscopies, where structural disorder was studied [2]. It is well-known that intense, short wavelength radiation, such as high brilliance synchrotron radiation, leads to radiation induced damage as well as charging of the deposited nanoparticle samples, which may significantly change their properties [3]. This is especially true for small nanoparticles and quantum dots. Charging and photoionization of nanoparticles involving outer electronic shells has been investigated in the past by experimental and theoretical approaches [4-6]. Charging of free nanoparticles by X-rays has been studied recently in an electrostatic precipitator, where most efficiently diffusion charging is observed in the dense gas phase that surrounds the particles [7]. Direct photoelectric charging is relatively weak under these conditions. Properties of nano- and microparticles are suitably investigated in traps over long time periods without any contact to a substrate [8-10]. This is of crucial importance for those properties, where contributions of the substrate dominate. Trap experiments also allow controlled charging using either electrons or ionizing radiation. In the case of insulators, charging may lead to substantial changes in electronic properties of matter [11].

We report in this work results on trapped nanoparti-

cles, which allow us to vary their charge state in a controlled way, by using tunable soft X-rays. First experiments on trapped, element-selectively excited nanoparticles are presented, where distinct changes in charge state are a result of direct photoelectric charging including the emission of secondary electrons. These results are used to derive charging mechanisms of free nanoparticles by soft X-rays.

The experimental setup consists of a three-dimensional electrodynamic trap, which serves for nanoparticle storage in an ultrahigh vacuum setup, with a base pressure  $< 10^{-8}$  mbar during the experiments. The trap consists of two conical cap electrodes and eight vertical rods, which replace the ring electrode of a classical three electrode Paul-trap [8,12]. The AC voltage of the driving field is applied to the cone electrodes. A small loudspeaker below the trap serves as a particle reservoir as well as a particle injector. It is filled with monodisperse SiO<sub>2</sub> particles (Merck) of  $498 \pm 36$  nm diameter [9]. The trapped particles typically carry initially some ten positive charges. They are illuminated by a frequency doubled Nd:YAG-laser ( $P < 50$  mW,  $\lambda = 532$  nm). The scattered light from the trapped particle is detected by an avalanche photodiode modulated by the secular motion frequencies  $\omega_r$  and  $\omega_z$  perpendicular and parallel to the trap axis, respectively. Both frequencies are obtained from a fast Fourier transform of the photodiode signal. This allows us to derive the charge-to-mass ratio  $Q/M$  of the particle [8,14]. Upon mass and charge state characterization the particles are exposed to monochromatic synchrotron

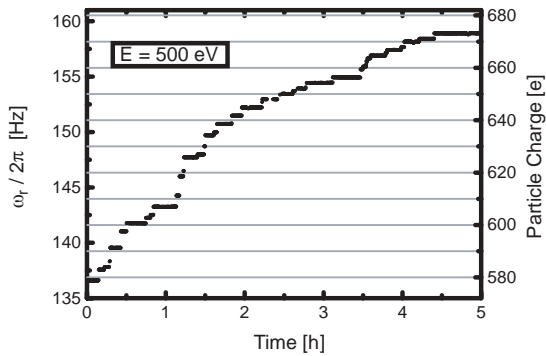


FIG. 1: Charge state of a trapped  $\text{SiO}_2$  nanoparticle of 500 nm diameter upon X-ray illumination (500 eV) as determined by its secular motion frequency  $\omega_r$  within an electrodynamic trap.

radiation in the soft X-ray regime (30-580 eV), using the U125/1-SGM- and UE52-SGM-beam lines at the storage ring BESSY-II (Berlin, Germany).

Fig. 1 shows a typical charging curve of a single trapped nanoparticle recorded at 500 eV photon energy. The charging curve shows distinct steps corresponding to changes in particle charge multiples of the elementary charge  $e$ . This occurs as a result of the absorption of soft X-ray photons. We safely assume that under these conditions, i.e. at low photon flux, just single photons hit the particle. Note that this situation is different, if the photon flux is increased (see below). The absence of downward steps in Fig. 1 indicates that at low charge state no charges are lost, e.g. by collisions with the residual gas or ion desorption.

Charging curves have been recorded at various photon energies ranging between 30 eV and 560 eV. Fig. 2 (a)-(h) shows a comparison of the step height distributions obtained from charging curves similar to that shown in Fig. 1. The charges on the particles are in each case  $< 800$ , corresponding to a surface potential of 0.25 - 4.9 V. The statistical analysis of the step heights yields the electron emission probability per absorbed photon. Note that the total  $4\pi$  solid angle integrated emission probability is determined. The results indicate that the average step height per absorbed photon increases as function of photon energy. This is straightforward since single ionization is expected to dominate at low photon energy, whereas double and multiple ionization occurs at increased photon energies, especially above the Si 2p-edge ( $E > 105$  eV). Fig. 2(a)-(c) have been recorded in the inner-valence regime, where single ionization dominates. All photon energies are well below the Si 2p-edge. There is already a finite probability for the emission of two electrons per absorbed photon, even at 30 eV (cf. Fig. 2(a)). This process is most likely due to the electron emission from different sites of the nanoparticle, where either secondary ionization of neighboring sites to

the absorbing center by the photoelectron [15] or fast charge transfer processes may occur [16]. Direct double ionization involving the emission of two correlated electrons is expected to be of weak cross section, similar to photoionization of atoms (cf. ref. [17]). Above the Si 2p-edge LMM-Auger processes become active, whereas in the O 1s-continuum KLL-Auger processes dominate. These lead efficiently to double and multiple ionization. Moreover, secondary electrons also contribute to an increase in particle charge. As a result, the step heights increase with photon energy, so that up to 7 charges per absorbed photon are observed (cf. Fig. 2(g)) and the intensity of the multiple ionization events increases with photon energy. The distribution of emitted secondary electrons per charging event is modeled by Poisson distributions, as indicated by full lines in Fig. 2. It is fitted to the experimental data by using  $\Delta Q \geq +2$ -events. The maximum of this function  $\delta$  is determined by the number of emitted charges divided by the number of charging events. A characteristic photon energy dependence of  $\delta$  is observed, corresponding to the average number of secondary electrons, which are emitted per absorbed photon, ranging between  $0.65 \pm 0.3$  and  $2.59 \pm 0.5$ , where the error limits are given by the limited number of charging events. The determined maximum of  $\delta \sim 2.6$  and its position at 500 eV agrees well with the reference value [18]. The Poisson distributions also show that there is a substantial probability for finding no change in charge state after photoabsorption. These events cannot be detected by the present experiment. Photoabsorption of soft X-rays without any change in particle charge appears to be quite possible, since inelastically scattered electrons may either get thermalized in the bulk of the particles or in the case of highly charged ones the secondary electrons may get trapped due to Coulomb attraction. The Poisson distributions appear to represent reasonable fits to the step height distributions for some photon energies. However, Fig. 2 (c)-(f), and (h) indicates that  $\Delta Q = +1$ -events are not suitably modeled by Poisson distributions. Further, the  $\Delta Q = +2$ -processes at 560 eV are also not well represented by the emission of secondary electrons. Intensity exceeding these distributions is marked by red color, reaching up to 40% of all emitted electrons. These processes are assigned to the emission of photoelectrons ( $\Delta Q = +1$ ) and KLL-Auger electrons ( $\Delta Q = +2$ ) (cf. Fig. 2(h)). They are evidently fast enough so that they can be emitted into the vacuum. In contrast, slow photoelectrons and LMM-Auger electrons do not contribute efficiently to charging. They are either formed at low photon energies in the inner-valence excitation regime ( $\leq 60$  eV) (cf. Fig. 2(a), (b)), near core ionization energies, i.e. near the Si 2p-edge (cf. Fig. 2(d)), and near the O 1s-edge (cf. Fig. 2(g)). Thus, we can easily distinguish from charging curves the ionization processes contributing to changes in particle charge, i.e. direct photoionization from ionization and relaxation via the emission of sec-

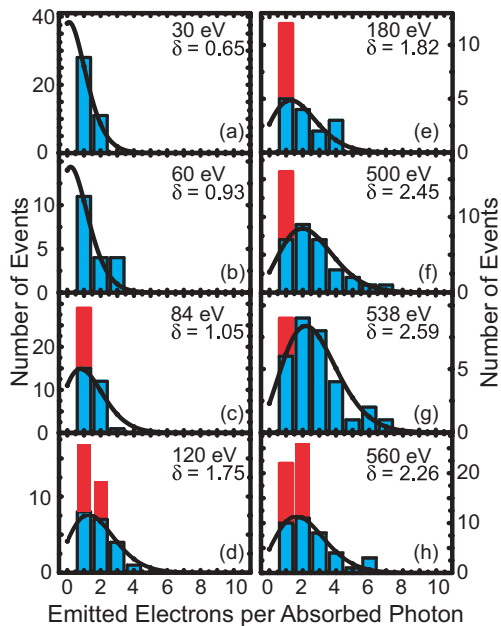


FIG. 2: Step height distributions from charging curves at different photon energies. The height of the bars is obtained from the experimental results (cf. Fig. 1). The solid lines correspond to Poisson distributions. These model the emission of secondary electrons, where  $\delta$  corresponds to the maximum of these distributions. Contributions from direct photoionization and KLL-Auger processes are indicated by red color.

ondary electrons. In all cases charging is predominantly due to the emission of secondary electrons.

Fig. 3 shows the photon energy dependence of three representative charging curves. Note that the particle charge is considerably higher than those displayed in Figs. 1 and 2. The primary experimental results are displayed in Fig. 3(a), where the photon flux is set, so that much faster changes in charge state occur compared to Figs. 1 and 2. As a result, no step-like structures can be resolved. The experiments start at a well-defined, initial charge state that is adjusted at 520 eV photon energy. Subsequently, the photon energy is increased, which leads to a further increase in particle charge. All curves show that the slope of the charge state changes significantly at the O 1s-edge, which is due to O 1s-absorption [19-22]. On the right hand side of Fig. 3(a) we have estimated the surface potential of the particle, assuming that all charges are located on the surface of the spherical particle. This indicates that the surface potential varies between 50 V and 420 V. The first derivative of the charging curves is shown in Fig. 3(b). These spectra are normalized to the photon flux so that they can be compared to each other. Furthermore, we have considered that the residual gas leads to a steady discharge of the particles at high charge states ( $Q > 40,000$ ), i.e. we observe in this regime only a net charging current. The results indicate that the resonant O 1s-excitation changes

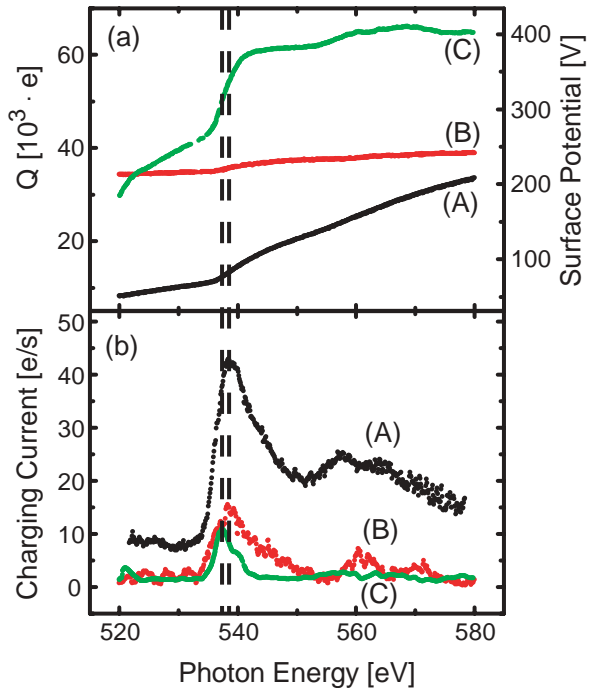


FIG. 3: (a) Charging curves as a function of photon energy of a differently charged SiO<sub>2</sub> nanoparticle; (b) First derivative of the results shown in (a), corresponding to the charging current as a function of photon energy in the O 1s-excitation regime. The vertical dashed lines indicate the position of the maximum in curve (A) and (C), respectively.

distinctly the charge state in SiO<sub>2</sub> nanoparticles. At the lowest particle charge (curve (A) in Fig. 3(b)) we observe the characteristic near-edge features of SiO<sub>2</sub> absorption [19-22]. The maximum of the major asymmetric feature is located at 538.6 eV. This energy is in agreement with previous work, where various molecular final states contribute to this strong absorption band [20]. We note that results from electron energy loss spectroscopy show this maximum near 535 eV [19], whereas in more recent *ab initio* work this band is moved to  $\sim 543$  eV [21]. Moreover, there is a broad continuum resonance with a double hump structure peaking near 557 eV and 564.5 eV, which has also been found in previous work [22].

Fig. 3(b) (curve (B)) shows that the intensity of the charging current has substantially decreased compared to curve (A), but the shape of the near-edge feature is still similar to that of curve (A). The intensity in the O 1s-continuum is decreased and the continuum resonances are barely visible. This indicates that considerably less charges are emitted from a particle that carries  $\sim 35,000$  charges. Evidently, the surface potential, which is estimated to 250 V, retains about 85% of the emitted charges. These are mostly slow electrons, which originate from inelastically scattered photoelectrons (secondaries) and Si LMM Auger electrons. All other electrons are expected to have sufficient kinetic energy to be emitted

above the vacuum level and contribute to the charging current and to an increase of the particle charge. Similarly, curve (C) shows that there is a further decrease in charging current, if the initial particle charge is increased to ca. 50,000 charges at 538 eV photon energy. As a result, only  $\sim 5\%$  of the electron charging current is observed in the O 1s regime compared to curve (A). There is hardly any charging current in the O 1s-continuum and the maximum of the intense resonance is redshifted by  $\sim 1$  eV relative to that shown in spectrum (A) (cf. vertical dashed lines in Fig. 3). We also note that the line profile is significantly narrower in spectrum (C) than in the other ones (A) and (B). This change in near-edge structure as a function of particle charge is assigned as follows: With increasing particle charge the surface potential retains electrons that are emitted after photoabsorption. Near the O 1s-edge electrons of different kinetic energy are produced, reaching from near zero kinetic energy electrons to fast ones of  $>500$  eV. The slow electrons which are suppressed at higher charge states come from shake-off processes as well as inelastically scattered photoelectrons, which come most likely from secondary electrons from the bulk. Fast electrons come either from normal and resonant Auger processes as well as direct outer shell photoionization. The latter process is of negligible cross section in the O 1s-regime and should not vary significantly across the absorption edge. Resonant Auger processes yield the fastest electrons, occurring only upon resonant excitation of pre-edge resonances. These electrons can still be emitted even at the highest surface potential and contribute to curve (C). Previous theoretical work indicates that there are three unoccupied states ( $T'$ ,  $T1$ , and  $A1$ ) that can be reached upon O 1s-excitation below 538 eV [20]. Evidently, the resonant Auger spectra of the transitions that contribute to the dominant near-edge feature have distinct properties, so that electrons of different kinetic energy are emitted, where the fastest ones are formed by excitation with photon energies ranging between 533 eV and 542 eV. Their magnitude is evidently too low so that they are not observed in the charging curve show in Fig. 2(g). The charging curve (C) shown in Fig. 3(b) reaches  $>60,000$  charges, corresponding to a surface potential of  $\sim 420$  V. This value is clearly lower than the photon energy used for charging in the O 1s-regime. It is evidently not reached since there are efficient charge loss mechanisms active, as mentioned above. On the other hand, a surface potential of  $\sim 420$  V cannot retain efficiently KLL-Auger electrons in the O 1s-continuum. This indicates limitations of the oversimplified model of charge localization on the surface of the spherical particle, used to determine the surface potential. The spectral changes observed in Fig. 3(b) require at least a surface potential of  $>500$  V in order to retain quantitatively all electrons from normal KLL-Auger pro-

cesses upon O 1s-ionization. It appears to be rather plausible that the charges are not uniformly distributed over the particle surface, so that defect sites can contribute to charge localization. Recent *ab initio* work indicates indeed, that twofold coordinated silicon atoms are hole traps in  $\text{SiO}_2$  [23].

In conclusion, we have investigated the charging mechanisms of free  $\text{SiO}_2$  nanoparticles that are selectively excited in the soft X-ray regime. The number of emitted electrons per absorbed photon changes significantly as a function of photon energy, indicating that both secondary electrons and primary photoelectrons contribute to particle charging by soft X-rays. Furthermore, the number of absorption events with effectively no electron ejection increases with the particle charge. Experiments in the O 1s-regime indicate that at low charge state the energy dependence of the charging current is similar to that of the photoabsorption of macroscopic  $\text{SiO}_2$ . At high particle charge only those electrons from resonant Auger processes can contribute to an increase of the charge state.

We thank A.A. Pavlychev for helpful discussions. Financial support by the Bundesministerium für Bildung und Forschung (BMBF) and the Deutsche Forschungsgemeinschaft are gratefully acknowledged.

- 
- [1] M.C. Daniel et al., Chem. Rev. **104**, 293 (2004).
  - [2] K.S. Hamad et al., Phys. Rev. Lett. **83**, 3474 (1999).
  - [3] H. Döllefeld et al., J. Chem. Phys. **117**, 8953 (2002).
  - [4] C. Delerue et al., Phys. Rev. Lett. **75**, 2228 (1995).
  - [5] L.-W. Wang et al., Phys. Rev. Lett. **91**, 056404 (2003).
  - [6] T.D. Krauss et al., Phys. Rev. Lett. **83**, 4840 (1999).
  - [7] P. Kulkarni et al., J. Aerosol Sci. **33**, 1279 (2002).
  - [8] S. Schlemmer et al., J. Appl. Phys. **90**, 5410 (2001).
  - [9] D. Gerlich, Hyperfine Interactions **146**, 293 (2003).
  - [10] S. Arnold et al., Rev. Sci. Instrum. **70**, 1473 (1999).
  - [11] N.H. Turner et al., Anal. Chem. **70**, 229R (1998).
  - [12] W. Paul, Rev. Mod. Phys. **62**, 531 (1990).
  - [13] S. Schlemmer et al., Appl. Phys. A **78**, 629 (2004).
  - [14] M. Grimm et al., AIP Conf. Proc. **705**, 1062 (2004).
  - [15] W. Biester et al., Phys. Rev. Lett. **59**, 1277 (1987).
  - [16] R. Santra et al., Phys. Rev. B **64**, 245104 (2001).
  - [17] N. Saito et al., Int. J. Mass Spectrom. **115**, 157 (1992).
  - [18] D.R. Lide (ed.), CRC Handbook of Chemistry and Physics, 74. Edition, CRC Press, Boca Raton, 1993, 12-107.
  - [19] Z.Y. Wu et al., J. Phys.: Cond. Matter **8**, 3323 (1996).
  - [20] I. Tanaka et al., Phys. Rev. B **52**, 11733 (1995); A. Marcelli et al., J. Phys. (Paris) **46**, C-8, 107 (1985).
  - [21] S.D. Mo et al., Appl. Phys. Lett. **78**, 3809 (2001).
  - [22] M. Taillefumier et al., Phys. Rev. B **66**, 195107 (2002).
  - [23] V.A. Gritsenko et al., Solid State Commun. **121**, 301 (2002).